STRESS-STRAIN ANALYSIS OF THE DIFFERENTIAL CAGE USING THE NUMERICAL SIMULATION MODEL

Tomáš Vrána*, Josef Bradáč**, Jan Kovanda***

The strength and stiffness of the differential cage is very important issue, because it affects the functionality of the other components of powered axles. The problem is that for the stress analysis of the differential cage is not possible to use conventional strength and elasticity approaches, because the differential cage has very complex geometrical shape and is also loaded by the combination of forces generated by the load engagement of the bevel gear. Therefore numerical simulations are more and more frequently used to solve this complex problem when the main task is creation the computational model that correspond the real state. The present paper deals with designing the computational model of the cage differential drive of the rear powered axle of utility vehicle. This model is then used for the strength structural analysis of the differential cage assembly. Presented computational model takes into account also the load of the differential cage thanks to the preload in strength bolts which join the bevel crown gear and differential cage.

Keywords: *FEM computational model, differential cage, rear powered axle, numerical simulation, stress-strain analysis*

1. Introduction

Commercial trucks usually use classic power scheme which means the engine in the front section and rear powered axle [7]. In the middle of the bridge axle is located the bevel gear drive and differential, which create the final gear and distribute the drive torque from the input axle through the right and left drive shaft to the vehicle wheels [10], Fig. 1.

The differential gear train mechanism is used to transmit the power from the engine-gear box system to the rear wheels of an automobile, and to rotate the rear wheels at different speeds while the automobile is taking a turn [1]. The differential is the transmission axle, with two degrees of freedom [9], which provides automatic balancing the different wheel speeds due to the different paths when the vehicle is driving in a curve, as it shown in Fig. 2. This functionality prevents introducing parasitic stress in axles and reduces the tire wear. From this perspective, it is a very important mechanism because its improper function may adversely affect the other parts of the vehicle transmission. There are many publications focused on the determination of the kinematic relationships of different designs of differentials, like [1, 5, 6]. The present paper deals with the strength and toughness analysis, which is a key issue in the engineering practice. For the powered rear axle of the truck is most commonly

* Ing. T. Vrána, Department of Vehicles and Ground Transport, Faculty of Engineering, CULS Prague, Kamýcká 129, 165 21 Praha ů Suchdol

** Ing. J. Bradáč, PhD., Department of Automotive Technology, ŠKODA AUTO University, Na Karmeli 1457, 293 60 Mladá Boleslav, Czech Republic

*** prof. Ing. J. Kovanda, CSc., Department of Security Technologies and Engineering, Faculty of Transportation Sciences, CTU in Prague, Konviktská 20, 110 00 Praha 1, Czech Republic

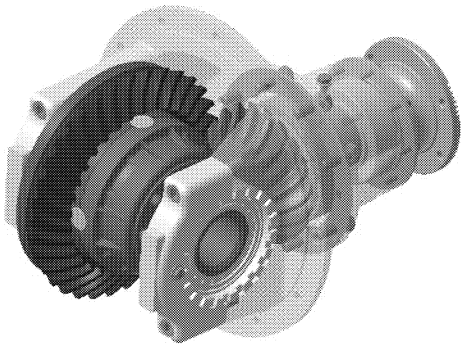

Fig.1: Bevel gear and the differential cage placed in the final gear [10]

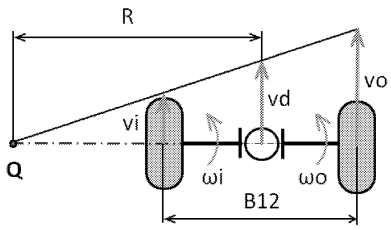

Fig.2: Differential operation during driving in a curve

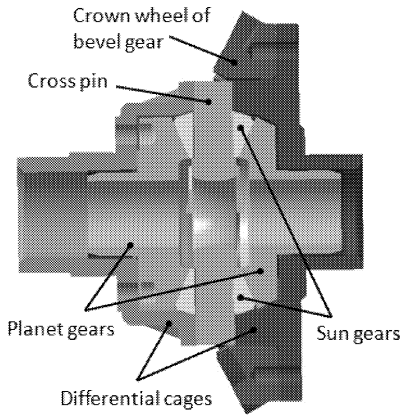

Fig.3: Schematic sectional view of a differential

used the conical differential with two planet wheels and four satellites which are arranged symmetrically on the differential cross pin, see Fig. 3. Kinematic differential ratio can be determined according [2].

If B_{12} is the wheels gauge, r_d tires dynamic radius, R the radius of the circle that circumscribes the axle centreline with the speed v_d, than the angular speed of the inner and outer wheel can be determined according to equations (1), (2).

$$\omega_\mathrm{i} = \frac{v_\mathrm{i}}{r_\mathrm{d}} = \frac{R - \dfrac{B_{12}}{2}}{r_\mathrm{d}\, R}\, v_\mathrm{d}\ , \tag{1}$$

$$\omega_\mathrm{o} = \frac{v_\mathrm{o}}{r_\mathrm{d}} = \frac{R + \dfrac{B_{12}}{2}}{r_\mathrm{d}\, R}\, v_\mathrm{d}\ . \tag{2}$$

The difference between angular speed $\omega_\mathrm{o} - \omega_\mathrm{i}$ of the inner and outer wheel is balanced thanks to the differential with the relative turning of planet gears (Fig. 3).

2. Computational model of the differential

For numerical calculations using finite element method the CAD model of differential cage was firstly created, see Fig. 4. Basic components are the bevel crown gear (1) and the left (2) and right (3) differential cage. Both differential cages are joined with eight bolts (4)

Component	Material		m [kg]	I_x [kg.m^2]	I_y [kg.m^2]	I_z [kg.m^2]
	Name [–]	Re_{min} [MPa]				
Bevel crown gear	16MnCr5	588	8.287	0.068	0.134	0.068
Left differential cage	15 230.7	835	14.719	0.077	0.142	0.077
Right differential cage	15 230.7	835	8.021	0.034	0.043	0.034

Tab.1: Weight and moments of inertia for individual components of the computational model

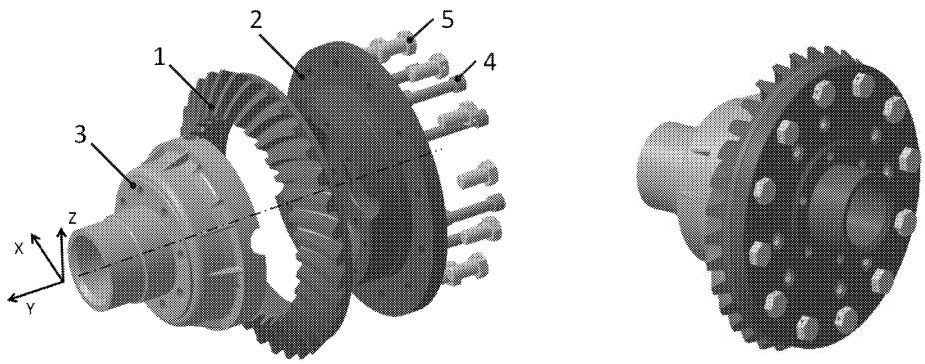

Fig.4: CAD model of the differential – disintegration view (left), assembly (right)

and the crown wheel on the left side with twelve bolts (5). The weight and moments of inertia I_x, I_y and I_z indexed to x, y, z axis for the individual assembly components shows Tab. 1.

Created computational model is supplemented by the boundary conditions describing statically determinate clamping of the left and right differential cage in ball bearings. The cylindrical surface of the right bearing cage cannot move in x and z direction and left cage in x, y, z direction. To create the physical contact between the individual assembly bodies the contact condition that prohibits the surface penetration of one body to another is applied. These structures provide transmission of deformation and force between assembly bodies. FEM volume mesh of the whole assembly is composed of linear tetrahedral elements. The resulting computational model has 299 308 elements and 69 432 node points.

The geometry of 3D model was created as the solid model in Catia V5. Than the package Hyperworks was used for the preparation of simulation mesh and evaluation of computational results. The main parts of this computational package are Hypermesh pre-processor, computational core RADIOSS and post-processor HyperView.

2.1. Force analysis of the differential cage

The differential cage is loaded by the tangent, radial and axial force that initiate in the bevel crown gear in computational point P, see Fig. 5. Crown wheel then transfers these forces to self differential cage. The size and orientation of forces in the bevel crown gear depends on gearing parameters (e.g. gearing angle β_p) but also on the orientation of the input torque moment. During the computation is important to respect two different loading states and thus the forward and reverse driving. Forces were always set for the maximum loading mode which means driving on the adhesion limit for defining axle load m_H (axle pressure), stated by legislation. For the forward driving the force effect can be determine according to [3] using the equations (3), (4) and (5).

Tangent force at crown wheel

$$F_{\mathrm{t}} = \frac{2\,M_{\mathrm{P}}}{d_{\mathrm{P1}}}\ . \tag{3}$$

Radial force at crown wheel

$$F_{\mathrm{r}} = F_{\mathrm{t}}\,\frac{\tan\alpha_{\mathrm{nP}}\,\cos\delta_2 + \sin\beta_{\mathrm{P}}\,\sin\delta_2}{\cos\beta_{\mathrm{P}}}\ . \tag{4}$$

Axial force at crown wheel

$$F_{\mathrm{a}} = F_{\mathrm{t}}\,\frac{\tan\alpha_{\mathrm{nP}}\,\sin\delta_2 - \sin\beta_{\mathrm{P}}\,\cos\delta_2}{\cos\beta_{\mathrm{P}}}\ . \tag{5}$$

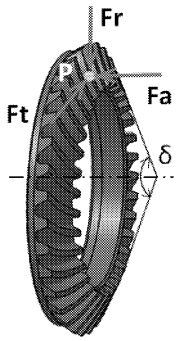

Fig.5: Forces at crown wheel during crowding (forward driving mode)

The differential cage is also loaded by the axial compression stress thanks to pre-stressing forces initiate by individual bolts that join the crown wheel and the left differential cage. The reason of this preload is to assure uni-axial tensile stress in bolts and thus prevent initiation of shear stresses. Thanks to that the fatigue lifetime of screwed joints can be prolonged. The equation for the pre-stressing force of one bolt of the crown wheel – left differential cage is possible to determine using (6).

$$Q = \frac{\dfrac{M_{\mathrm{p}}\,i_{\mathrm{ST}}}{f\,\dfrac{D_{\mathrm{s}} + d_{\mathrm{s}}}{4}}}{i_{\mathrm{S}}}\ . \tag{6}$$

The individual force values for the maximal weight capacity of one axle $m_{\mathrm{H}} = 11\,500\,\mathrm{kg}$ and $13\,000\,\mathrm{kg}$ are shown in the Table 2. These resulting values are then used as boundary conditions for numerical calculations.

Loading effect of differential cage		Loading of differential cage			
		Forward driving		Reverse driving	
		11 500 kg	13 000 kg	11 500 kg	13 000 kg
Tangent force at crown wheel	F_{t} [N]	105 473	149 034	105 473	149 034
Radial force at crown wheel	F_{r} [N]	95 577	135 050	46 998	66 408
Axial force at crown wheel	F_{a} [N]	1 149	1 626	83 232	117 606
Preload of bolts	Q [N]	64 421	72 786	64 421	72 786

Tab.2: Force analysis of differential cage

3. Results of the stress analysis

For each element of the computational model the stress tensor $\{\sigma_x, \sigma_y, \sigma_z, \tau_{xy}, \tau_{xz}, \tau_{yz}\}$ was determined. This tensor composes of six elements. Three represent normal stresses σ and the rest three shear stresses τ [4, 8]. The reduced stress using 'von Mises' hypothesis is then calculated according to equation (7).

$$\sigma_{\mathrm{red,Mises}} = \sqrt{\frac{1}{2}\left[(\sigma_x - \sigma_y)^2 + (\sigma_x - \sigma_z)^2 + (\sigma_y - \sigma_z)^2 + 6\left(\tau_{xy}^2 + \tau_{xz}^2 + \tau_{yz}^2\right)\right]} \ . \tag{7}$$

The result of stress analysis of the differential cage of the rear powered axle is then the reduced stress and strain field. Maximal stress and strain values are also important for the investigation of the stress and stiffness level of studied differential cage. Results of stress-strain analysis are shown in Table 3.

Loading mode of differential cage

	Loading mode of differential cage			
	Forward driving		Reverse driving	
	11 500 kg	13 000 kg	11 500 kg	13 000 kg
Maximal global stress [MPa]	468	529	533	603
Maximal global deformation [MPa]	0.202	0.228	0.294	0.332
Maximal stress – bolts holes [MPa]	348	393	339	383
Maximal strain – bolts holes [mm]	0.117	0.131	0.134	0.332
Safety factor to yield strength [–]	1.78	1.58	1.57	1.38

Tab.3: Results of stress-strain analysis of differential cage

Different orientation and size of forces in the bevel gearing crown wheel load mode during forward and reverse driving causes the different values of maximum stress respectively the deformation of the differential cage. It is also possible to notice that the maximal stress values are placed in different areas. Stress distribution in the differential cage for the forward driving is shown in Figures 6, 7 and 8. The same situation for the reverse driving is shown in Figures 9, 10 and 11.

Maximal global stress for the forward driving is found in a fit of casting for the installation of the crown wheel, see Fig. 6. Contrary the maximal global stress for reverse driving is in the area of radial hole for receiving the differential cross pin. Maximal stresses do not reach the yield strength of used materials and the permanent strains do not occur. Strain fields are displayed in Figures 7 and 10. In the forward driving mode of the vehicle the larger area of the left cage flange is affected in comparison to the reverse driving mode. The crown wheel is joined to this flange. Results show that stresses and strains in the differential cage assembly are higher for the reverse driving mode and lower for the forward driving mode. The maximal stress is about 14 % higher and the maximal strain about 45 %. The most stressed part of the differential is the left cage. If the weight capacity is increasing from 11 500 kg to 13 000 kg the strain value is higher at about 13 %.

Comparative model with the differential load without preloading forces of the crown wheel bolt – left differential cage was also calculated. It was investigated that these forces influence only the local stress of the differential cage around the screw and resulting calculated values do not reach the maximum global value.

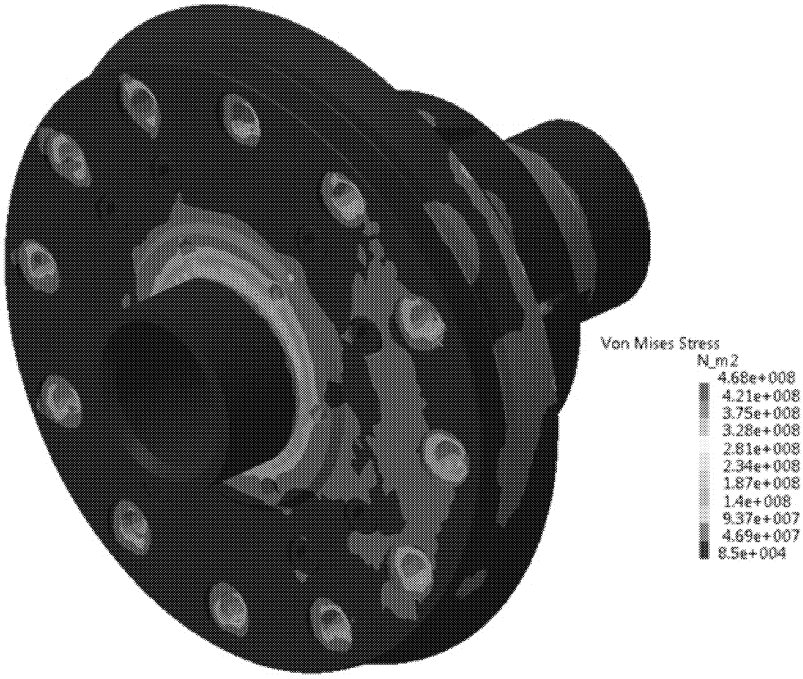

Fig.6: Stress field in differential cage (using 'von Mises' hypothesis) – forward driving, maximal weight capacity for one axle 11 500 kg, left view

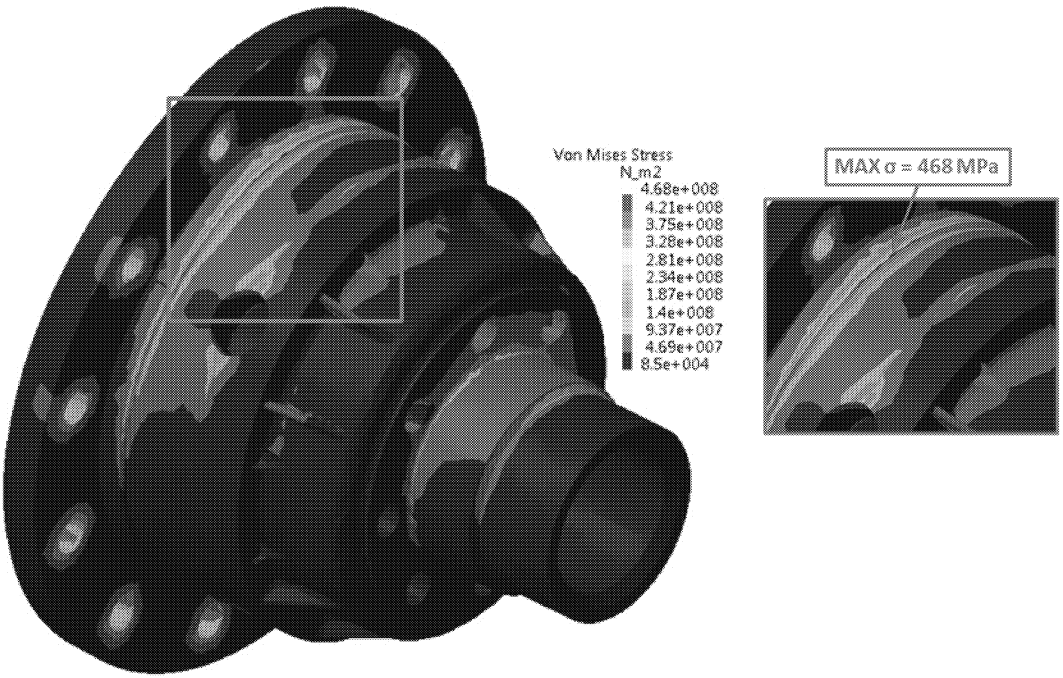

Fig.7: Stress field in differential cage (using 'von Mises' hypothesis) with the detail of the maximal stress – forward driving, hidden crown wheel, maximal weight capacity for one axle 11 500 kg, right view

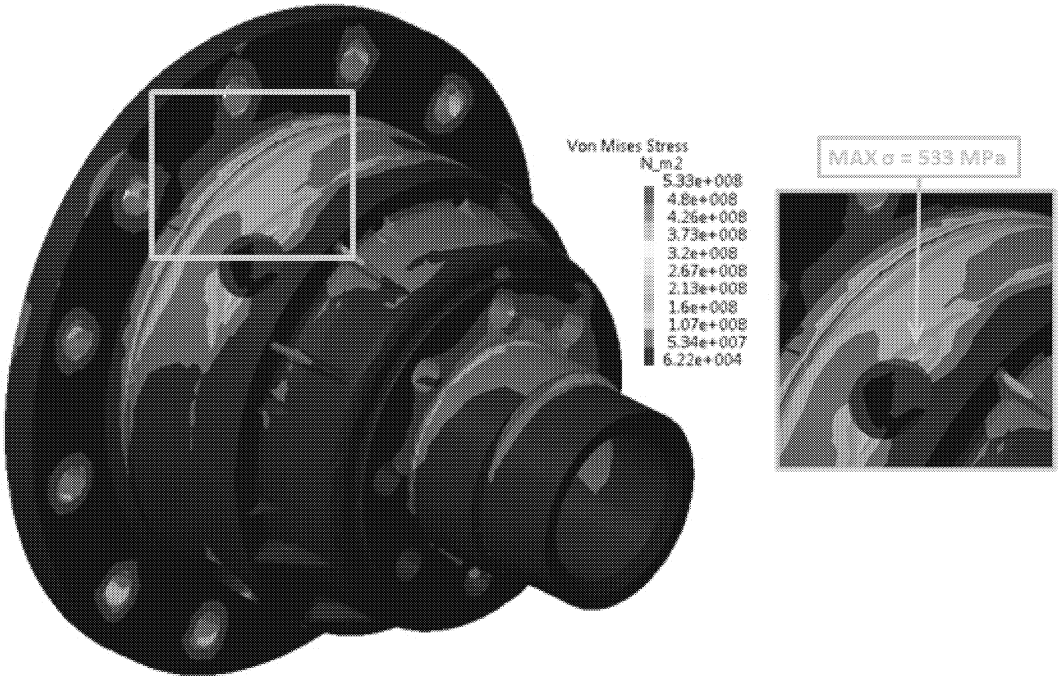

Fig.8: Strain field in differential cage – forward driving, maximal weight capacity for one axle 11 500 kg, left view

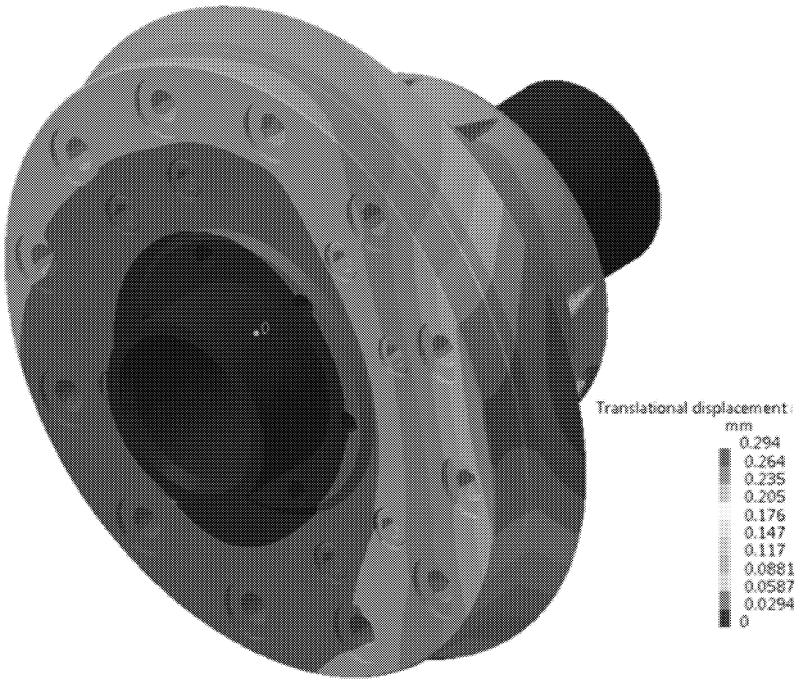

Fig.9: Stress field in differential cage (using 'von Mises' hypothesis) – reverse driving, maximal weight capacity for one axle 11 500 kg, left view

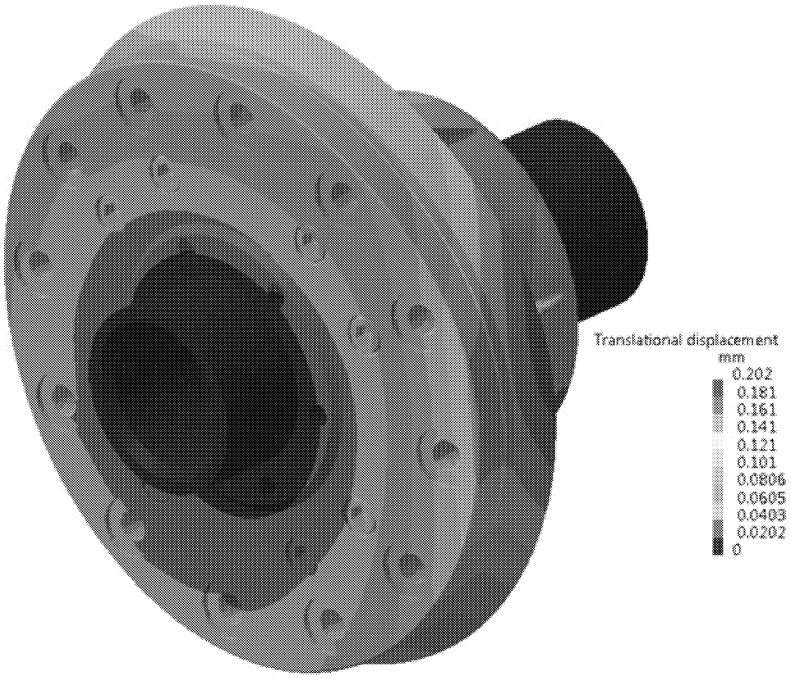

Fig.10: Stress field in differential cage (using 'von Mises' hypothesis) with the detail of the maximal stress – reverse driving, hidden crown wheel, maximal weight capacity for one axle 11 500 kg, right view

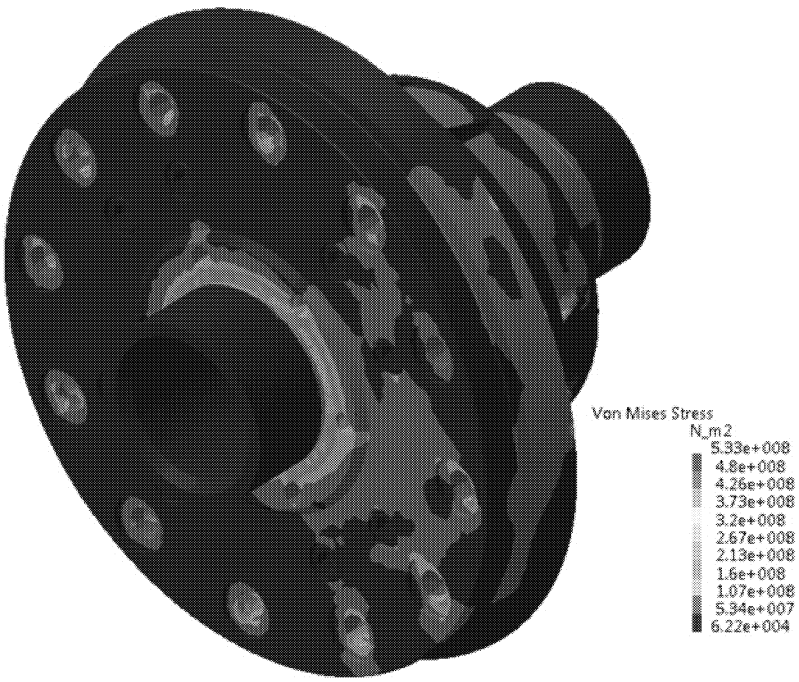

Fig.11: Strain field in differential cage – reverse driving, maximal weight capacity for one axle 11 500 kg, left view

4. Conclusion

The stress-strain analysis of differential cage of the rear powered axle of utility vehicle using FEM simulation model was introduced in the paper. Simulation model was prepared as an assembly of individual components like the bevel gear, the left and right differential cage and joining bolts. The computational model was completed with the boundary condition concerning kinematic structures between the individual bodies. Prepared model was subsequently loaded with forces that arise during gearing. Moreover the additional load causes by the preload in bolts joining the differential cage and crown wheel was also simulated. The stress analysis was investigated for different limits of the maximal weight capacity of an axle and also for different driving conditions which means the forward and reverse driving. Acquired results are reduced stresses and strains corresponding to the particular conditions. Results show that the differential cage is more loaded in case of the reverse driving whereas the stress values increasing continuously also with the weight capacity limit. Furthermore it was investigated that the left differential cage is more loaded than the right one. The maximal stress values for all computed cases are under the yield strength limit of used materials. From this results that computed strains are in this case elastic and probability of rupture is minimal.

Nomenclature

B_{12}	Wheel gauge	[m]
v_{i}	Circumferential speed of inner wheel	[m/s]
v_{o}	Circumferential speed of outer wheel	[m/s]
ω_{i}	Angular speed of inner wheel	[rad/s]
ω_{o}	Angular speed of outer wheel	[rad/s]
v_{d}	Angular speed of axle centre	[m/s]
r_{d}	Dynamical radius of tire	[m]
R	Curve radius	[m]
m_{H}	Maximal effective weight for axle	[kg]
M_{P}	Moment at pinion – bevel gear	[Nm]
Q	Biasing force of the bolt ring gear ů differential cage	[N]
i_{ST}	Permanent transfer gear	[–]
f	Friction coefficient	[–]
D_{s}	Outer diameter of crown wheel – differential cage	[mm]
d_{s}	Inner diameter of crown wheel – differential cage	[mm]
P	Computational point of bevel gear	[–]
i_{s}	Number of bolts	[–]
F_{t}	Tangent force at crown wheel	[N]
F_{r}	Radial force at crown wheel	[N]
F_{a}	Axial force at crown wheel	[N]
d_{P1}	Middle spacing diameter of pinion gear	[N]
β_{P}	Slope angle of gearing in point P	[°]
δ_2	Cone angle of crown wheel	[°]
α_{nP}	Gearing angle in computational point P	[°]
m	Weight	[kg]
Re_{min}	Minimal yield strength	[MPa]
I_{x}	Moment of inertia in direction of x axis	[kg.m^2]
I_{y}	Moment of inertia in direction of y axis	[kg.m^2]
I_{z}	Moment of inertia in direction of z axis	[kg.m^2]
σ_{x}	Normal stress in direction of x axis	[MPa]

σ_{y}	Normal stress in direction of y axis	[MPa]
σ_{z}	Normal stress in direction of z axis	[MPa]
τ_{xy}	Shearing stress in plane xy	[MPa]
τ_{xz}	Shearing stress in plane xz	[MPa]
τ_{yz}	Shearing stress in plane xz	[MPa]

References

[1] Goyal S., Vaz A.: Modeling and Simulation of Dynamics of Differential Gear Train Mechanism using Bond Graph, Proceedings of the 1st International and 16th National Conference on Machines and Mechanisms (iNaCoMM2013), IIT Roorkee, India, Dec 18–20 2013

[2] Vlk F.: Technical automobile handbook, publisher Vlk, 1st edition, Brno 2003, ISBN 80-238-9681-4

[3] Švec V.: Machine parts and mechanisms – Mechanical gears, Prague, ČVUT in Prague 2003, 174 p., ISBN 80-01-01934-9

[4] Michalec J. a kol.: Flexibility and strength I, Prague 1995, ČVUT in Prague, 320 p., ISBN 8001013332

[5] Draou A.: A Simplified Sliding Mode Controlled Electronic Differential for an Electric Vehicle with Two Independent Wheel Drives, Energy and Power Engineering, 2013, 5, 416–421, published online August 2013 (http://www.scirp.org/journal/epe)

[6] Zebrowski Z., Miroslaw T.: Modeling and simulation of tractor differential mechanism, 2013

[7] Vrána T.: Use of finite element method in the development of truck chassis for example stress analysis of the rear axle beam, International conference of young scientists, Prague 2014, 9.–10. 09. 2014, ISBN 978-80-213-2476-3

[8] Řezníček J., Řezníčková J.: Elasticity and strength in technical practice – Example III, Prague 2008, ČVUT in Prague, ISBN 978-80-01-03947-2

[9] Ambekar A.G.: Mechanism and machine theory, New Delphy 2007, Prentice Hall of India private limited, ISBN 978-81-203-3134-1

[10] Vrána T.: Complex design of rear drive axle for mixed traffic – master thesis, Prague 2009, ČVUT in Prague

Received in editor's office: April 14, 2015
Approved for publishing: June 1, 2015